International Journal of Pharmaceutics 368 (2009) 129–137

Contents lists available at ScienceDirect

International Journal of Pharmaceutics

journal homepage: www.elsevier.com/locate/ijpharm

Particle engineering using sonocrystallization: Salbutamol sulphate for pulmonary delivery

Ravindra S. Dhumal[a], Shailesh V. Biradar[a], Anant R. Paradkar[a,b,*], Peter York[b]

[a] Department of Pharmaceutics, Bharati Vidyapeeth University, Poona College of Pharmacy and Research Centre, Erandawane, Pune 411 038, Maharashtra, India
[b] Institute of Pharmaceutical Innovations, University of Bradford, Bradford, West Yorkshire BD7 1DP, UK

ARTICLE INFO

Article history:
Received 8 April 2008
Received in revised form 25 August 2008
Accepted 8 October 2008
Available online 18 October 2008

Keywords:
Sonocrystallization
Dry powder inhaler
Particle engineering
Salbutamol sulphate

ABSTRACT

The aim of present work was to produce fine elongated crystals of salbutamol sulphate (SS) by sonocrystallization for pulmonary delivery and compare with micronized and spray dried SS (SDSS) for *in vitro* aerosolization behavior. Application of ultrasound during anti-solvent crystallization resulted in fine elongated crystals (sonocrystallized SS; SCSS) compared to aggregates of large irregular crystals obtained without sonication. Higher sonication amplitude, time, concentration and lower processing temperatures favored formation of smaller crystals with narrow particle size distribution (PSD). SCSS was separated from dispersion by spray drying in the form of loose aggregates (SD-SCSS). The fine particle fraction (FPF) of formulations with coarse lactose carrier in cascade impactor increased from 16.66% for micronized SS to 31.12% for SDSS (obtained by spray drying aqueous SS solution) and 44.21% for SD-SCSS, due to reduced cohesive/adhesive forces and aerodynamic size by virtue of elongated shape of crystals. SD-SCSS was stable without any change in crystallinity and aerodynamic behavior for 3 months at 40 °C/75% RH, but amorphous SDSS showed recrystallization with poor aerosolization performance on storage. Sonocrystallization, a rapid and simple technique is reported for production of SS crystals suitable for inhalation delivery.

1. Introduction

Advances in drug delivery systems require specially engineered drug particles to meet biopharmaceutical (Blagden et al., 2007) and processing needs (York, 1999). Accordingly development of engineered drug particles has become major research due to limitations of conventional particle formation and pretreatment processes in fine-tuning the required characteristics. Techniques such as micronization (Ticehurst et al., 2000), spray drying (Ambike et al., 2004; Chawla et al., 1994), spray freezing (Hu et al., 2002), supercritical fluid processing (Schiavone et al., 2004), spherical crystallization (Nocent et al., 2001), solution atomization and crystallization by sonication (SAXS) (Kaerger and Price, 2004), sonocrystallization (Luque de Castro and Priego-Capote, 2007; Dhumal et al., 2008b) and melt sonocrystallization (Maheshwari et al., 2005; Paradkar et al., 2006) are introduced to provide particles with novel physicochemical properties.

Dry powder inhaler (DPI) formulations require drug particles with aerodynamic particle size below 5 μm for deep lung deposition along with good flow properties to ensure accurate dose metering. The choice and design of processing technique is vital in manipulating macroscopic shape and mesoscopic surface topography of particles. These properties play a critical role in determining flow, deaggregation and dispersion of fine particulates. Jet-milling micronization is the most frequently used technique to obtain particles with optimal respirable size from DPI formulations. However, micronization is energy intensive, time consuming and can introduce impurities into the product (Waltersson and Lundgren, 1985). The process also shows some disadvantages in practice such as inadequate control of particle size, undesired particle shape, surface charge modifications, decreased crystallinity and possible chemical degradation (Briggner et al., 1994; Ticehurst et al., 2000). Micron-sized spherical particles in respirable size can also be prepared by spray-drying of a drug solution (Chawla et al., 1994). However, spray drying yields amorphous product which is thermodynamically unstable and therefore show tendency to absorb moisture, agglomerate and recrystallize on storage (Chawla et al., 1994; Buckton et al., 1995).

Conventional anti-solvent crystallization with mechanical agitation has also been explored for crystal engineering. Poor-mixing leads to heterogeneous growth of crystals and in turn variation in

* Corresponding author at: Department of Pharmaceutics, Bharati Vidyapeeth University, Poona College of Pharmacy and Research Centre, Erandawane, Pune 411 038, Maharashtra, India. Tel.: +91 20 2543 7237; fax: +91 20 2543 9383.
E-mail address: arparadkar@rediffmail.com (A.R. Paradkar).

0378-5173/$ – see front matter © 2008 Elsevier B.V. All rights reserved.
doi:10.1016/j.ijpharm.2008.10.006

the particle size and morphological features (Zeng et al., 2001). Application of ultrasound during crystallization is known to avoid this by maintaining reasonably uniform conditions throughout the crystallization vessel (Louhi-Kultanen et al., 2006). Application of power ultrasound to control crystallization from solution is known as sonocrystallization (Guo et al., 2005; Luque de Castro and Priego-Capote, 2007). Ultrasound irradiation is commonly known to induce acoustic streaming, micro streaming and highly localized temperature and pressure within the fluid, these effects bring considerable benefits to crystallization process, such as rapid induction of primary nucleation, reduction of crystal size, inhibition of agglomeration and manipulation of crystal size distribution (Guo et al., 2005; Luque de Castro and Priego-Capote, 2007). As the number of primary nuclei increases, amount of solute on each primary nucleus decreases, thus decreasing the size of final crystal (Louhi-Kultanen et al., 2006).

In our previous attempt, we have obtained porous and sintered particles of ibuprofen and celecoxib by melt sonocrystallization, but the particles were unsuitable for inhalation due to higher size, hardness and density (Maheshwari et al., 2005; Paradkar et al., 2006). Kaerger and Price (2004), have demonstrated the potential of SAXS technique for production of uniform, spherical crystalline particles within a narrow PSD suitable for DPI. Traditionally, non-spherical particles have been avoided for potential problems of powder flow. However, the respirable fraction of drugs is reported to improve with the elongation ratio, as aerodynamic diameter shows a relatively small dependence on the length but is strongly correlated to the short dimension of the particles (Ikegami et al., 2002; Larhrib et al., 2003a).

In present work, we report application of sonocrystallization to produce fine needles of SS, separated by spray drying to obtain oval aggregates suitable for inhalation and evaluated for solid state characterization and aerosol performance in comparison with micronized SS and product obtained by spray drying SS aqueous solution (SDSS).

2. Materials and methods

2.1. Materials

The unprocessed SS and micronized SS were gift sample from Cipla Ltd., Mumbai, India and used as received. Lactose monohydrate (Pharmactose 200M, DMV International, The Netherlands), Rotahaler® (Cipla, Mumbai, India) and Hard gelatin capsules (Universal Capsules, Mumbai, India) were received as gift sample. Iso-propyl alcohol (IPA) of analytical grade was purchased from Merck, India.

2.2. Crystallization procedure

2.2.1. Sonocrystallization

In this study, the equipment consisting of a probe and sonifier (Sonics and Materials Inc., Vibra Cell, Model VCX 750, Connecticut, USA) was used. A probe (tip diameter 13 mm) was immersed 5 mm in the processing liquid. The device operates at a fixed wavelength of 20 kHz and is capable of inducing a maximum power output of 750 W, providing control over temperature. Predetermined amount of unprocessed SS was dissolved in 10 ml water and filtered through 0.45 μm pore size membrane. SS solutions were poured in 200 ml IPA placed in a 500 ml jacketed glass sonoreactor with ultrasonic irradiation by varying temperature, time and amplitude (Table 1). The resultant dispersion containing SCSS was collected and immediately characterized for particle size analysis. A control experiment was conducted with mechanical stirring instead of sonication to obtain PPT-SS particles.

2.2.2. Spray drying

The SCSS dispersion of batch with optimum particle size and PSD was immediately dried on a Twin cyclone Lab Spray Drier (LU-222 Advanced Model, Labultima, Mumbai, India), under following set of conditions: inlet temperature 130 °C, outlet temperature, 85 °C, feed rate 4–6 ml/min, atomization air pressure 1 kg cm^{-2} and aspiration pressure −200 mmWC to obtain SD-SCSS.

Aqueous SS solution (10%, w/v) was spray dried at parameters based on work of Chawla et al. (1994), to produce SDSS. The powders were transferred into a sealed container and stored over silica gel until further used for characterization.

2.3. Micromeritic properties

2.3.1. Particle size distribution

Particle size was measured by Laser Diffractometer, Mastersizer 2000 Ver. 2.00 (Malvern Instruments, Malvern, UK). Analysis was done in triplicate and mean results are presented. IPA was used as dispersant and obscuration was not less than 10% for each measurement. Particle size analysis was based on the refractive index (RI) of SS (1.553), and RI of IPA (1.378). The size distribution was expressed by the volume median diameter (VMD) and span. Span is a measure of the polydispersity of the PSD, defined as the difference in the particle diameters at 10 and 90% cumulative volume, divided by the VMD. Data analysis was done by Malvern Software Ver 3.0.

2.3.2. Particle morphology

Freshly prepared SCSS and PPT-SS dispersions were dropped on a glass slide and allowed to evaporate. The glass was then fixed on aluminum stubs using double sided adhesive tape, while unprocessed SS, micronized SS, SDSS and SD-SCSS samples were directly mounted on the aluminum stub. All samples were coated with a thin gold-palladium layer by Auto fine coater (Jeol, JFC, Tokyo, Japan). The surface topography was analyzed with a scanning electron microscope (Jeol, JSM-6360, Tokyo, Japan) operated at an acceleration voltage of 10 kV.

2.3.3. Powder flow

The static powder flow was characterized using Carr's compressibility index (CI), determined from the tapped (ρ_{tap}) and bulk densities (ρ_{bulk}) using following formula:

$$CI = \frac{\rho_{tap} - \rho_{bulk}}{\rho_{tap}} \times 100$$

Bulk density was determined by filling the powder in a 10-ml measuring cylinder, and tapped density was measured using tap density tester (ETD-1020, Electrolab, Mumbai, India) following 500 taps, which allowed the density plateau. Lower CI values are indicative of better flow behavior.

2.4. Moisture content determination

To determine moisture content of the powders, thermogravimetric analysis was performed using TA-60WS Thermogravimetric analyzer (Shimandzu, Japan). Samples (approximately 30–40 mg) were heated in platinum crucible in nitrogen atmosphere and the loss of mass as a function of temperature was recorded in triplicate.

Table 1
Summary of experimental conditions, VMD and span obtained by laser diffraction method.

Batch code	Sonication amplitude (%)	Temp. (°C)	Time (min)	SS conc. (mg/ml)	VMD (μm)[a]	Span[a]
1	25	5	3	250	3.1 ± 0.11	2.5 ± 0.10
2	50	5	3	250	1.8 ± 0.10	1.8 ± 0.91
3	75	5	3	250	1.6 ± 0.11	1.6 ± 0.89
4	50	15	3	250	5.1 ± 0.14	1.8 ± 0.97
5	50	25	3	250	7.2 ± 0.16	4.0 ± 0.18
6	50	5	1	250	8.1 ± 0.14	2.4 ± 0.96
7	50	5	5	250	1.6 ± 0.10	1.7 ± 0.92
8	50	5	3	150	9.9 ± 0.13	3.9 ± 0.14
9	50	5	3	200	6.8 ± 0.12	3.1 ± 01.5
10	50	5	3	275	3.8 ± 0.12	2.7 ± 0.91
SD-SCSS	50	5	3	250	1.6 ± 0.10	1.6 ± 0.78
PPT-SS	Stirring	5	30	250	22.3 ± 2.55	4.7 ± 0.21
Micronized SS	–	–	–	–	3.7 ± 2.85	3.3 ± 1.60

[a] Mean ± S.D., $n = 3$.

2.5. Diffuse reflectance infrared Fourier transform spectroscopy (DRIFTS)

The DRIFT spectra were obtained, after appropriate background subtraction using an FTIR spectrometer (FTIR-8400, Shimadzu Corporation) equipped with a diffuse reflectance accessory (DRS-8000, Shimadzu Corporation) and a data station. Powder samples of unprocessed SS, SDSS and SD-SCSS were mixed with dry potassium bromide and scanned from 4000 to 400 cm^{-1}.

2.6. Characterization of polymorphic form

2.6.1. Differential scanning calorimetry (DSC)

DSC studies were carried out using Mettler-Toledo DSC 821^e instrument equipped with an intracooler (Mettler-Toledo, Switzerland). Indium and Zinc standards were used to calibrate the DSC temperature and enthalpy scale. The samples were hermetically sealed in aluminum pans and heated at a constant rate of 10 °C/min over a temperature range of 25–220 °C. Inert atmosphere was maintained by purging nitrogen gas at flow rate of 50 ml/min.

2.6.2. X-ray powder diffraction (XRPD)

The XRPD patterns were recorded on X-ray diffractometer (D8 Advance, Bruker AXS Inc., Madison, USA). Samples were irradiated with monochromatized Cu Kα radiation (1.542 Å) and analyzed at 5–30° 2θ, step size: 0.02, time per step: 2 s. The voltage and current used were 30 kV and 30 mA, respectively.

2.7. Stability studies

The accelerated stability of SDSS and SD-SCSS samples was checked as per ICH guidelines at 40 ± 2 °C and 75 ± 5% RH up to 3 months. Samples were removed periodically (1, 2 and 3 months) and checked for crystallinity using DSC and XRPD. Three-month stability samples were checked for aerosolization performance after blending with coarse lactose carrier and compared with fresh samples.

2.8. Aerosol performance

The blends containing drug and coarse lactose, in the ratio 1:67.5, w:w were obtained by blending the micronized SS, SDSS and SD-SCSS with sieved fraction of coarse lactose (CL) monohydrate (between 63 and 90 μm). The CL was collected by sieving lactose monohydrate through 90 and 63 μm aperture sieves (Jayant test sieves, Mumbai, India) for 15 min each. The blending was carried out by sequential mixing of CL to either micronized SS, SDSS or SD-SCSS in stoppered vials placed on a vibromixer for 5 s till the desired ratio was obtained followed by final blending in a fabricated double cone blender for 30 min at 40 rpm. Content uniformity was determined across each blend spectrophotometrically at 276 nm (UV-1601, Shimandzu Corporation, Japan). Hard gelatin capsules (size "3") were filled with 33.0 ± 1.5 mg of the powder mixture so that each capsule contained 481 ± 20 μg SS, which was similar to the unit dose contained in a Ventolin Rotacap®. The filling was performed manually.

The dispersion behavior of the powders was assessed using an eight stage, nonviable cascade impactor with a preseparator (Graseby-Andersen, Atlanta, GA, USA) operating at a flow rate of 28.3 l/min measured with a rotameter (Gilmont, USA, GF-2005). The powder samples in capsules were aerosolized using Rotahaler® (Cipla Ltd., Mumbai, India). The capsule to be tested was placed in the inhaler device (Rotahaler), which had been fitted into a moulded rubber mouthpiece attached to the throat piece of the impactor. Once the assembly had been checked and found to be airtight and vertical, the pump was switched on, the dose released and the pump allowed to run for 10 s at 28.3 l/min before switching off. The capsule shell was then removed from the inhaler device and the deposition test was repeated so that nine more capsules were actuated in the same manner. The capsule shells and inhaler device were washed with the water and the solution was made up to a fixed volume. Each stage of the impactor was washed individually and the solution was made up to fixed volume. All the samples obtained were analyzed for salbutamol sulphate spectrophotometrically at 276 nm (UV-1601, Shimandzu Corporation, Japan).

A variety of parameters were employed to characterize the deposition profiles of SS. The recovered dose (RD) was the sum of the drug collected from capsule, inhaler device, preseparator, induction port and all stages of the impactor. The emitted dose (ED) was the amount of drug released from the inhaler device, i.e. the sum of drug collected at preseparator, induction port and all stages of the impactor. Fine particle dose (FPD) was defined as the amount of drug deposited on the stages 2 and below of the impactor. The fine particle fraction (FPF) was calculated as the ratio of FPD to RD. The total recovery (% recovery) of the drug was assessed by the ratio of the RD to the theoretical dose, the later being the dose of SS in the capsules. The theoretical dose of SS in one capsule was 481 ± 20 μg, which was equivalent to the filling weight of SS and lactose blends (33.0 ± 1.5 mg). The mass median aerodynamic diameter (MMAD) was calculated as the 50th percentile of the aerodynamic particle size distribution by mass. The geometric standard deviation (GSD) was calculated as square root of the ratio of the particle size at the 84.13th percentile to the 15.87th percentile. Both MMAD and GSD were determined from the linear region of the plot of the cumulative mass distribution as a function of the logarithm of aerodynamic diameter.

3. Results and discussion

During preliminary studies, when anti-solvent crystallization was carried out with stirring instead of sonication (Batch PPT-SS) the yield could not be improved beyond 61% (w/w) even after stirring for 30 min. While, when sonication was applied during anti-solvent crystallization (sonocrystallization) the induction of crystallization and crystal growth was faster indicating the definite effect of insonation on the induction of nucleation and crystal growth. During the process of sonocrystallization, concentration of SS solution, amplitude of sonication, duration of sonication and processing temperature were found to influence the time of precipitation and overall crystal growth. Therefore, to understand the contribution of these variables on the crystal size, shape and morphology various batches were designed by varying sonication amplitude, time, processing temperature and concentration of SS solution (Table 1). The product yield for all batches carried out with sonication varied from 92 to 96% (w/w) indicating good recovery with insignificant losses.

3.1. Micromeritic properties

3.1.1. Particle size distribution

Range of ultrasonic amplitudes (25, 50 and 75%) was tested in order to determine the optimum amplitude (Batches 1–3) and compared with PPT-SS. Fig. 1 shows the particle size distribution of PPT-SS and batches after sonication with different amplitudes at 5 °C, sonicated for 3 min after addition of 250 mg/ml SS solution. PPT-SS showed VMD of 22.3 μm with broad PSD as indicated by the higher span value (Table 1). Poor micro-mixing during anti-solvent process leads to accidental zones of supersaturation, heterogeneous growth of crystals, aggregation of particles and in turn variation in the particle size. As amplitude increases particle size and span was found to decrease. This decrease in particle size can be attributed to the intensified micro-mixing leading to enhanced mass transfer and diffusion between solvent and anti-solvent, which induced instantaneous high levels of supersaturation and resulted in rapid nucleation. As the number of primary nuclei increases, the amount of solute depositing on each primary nucleus decreases, thus decreasing the size of final crystal. Micronized SS also showed VMD of 3.7 μm, but the span (3.3) indicated the broad distribution of particle size. Increasing the power output from 50 to 75% resulted in similar results. Therefore, further experiments were carried out at 50% amplitude.

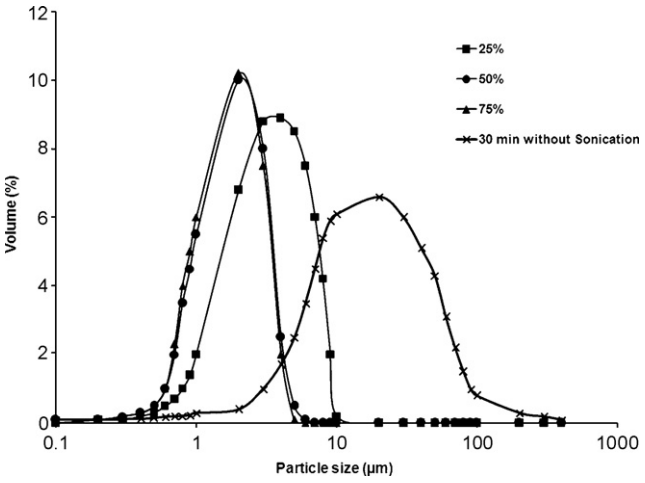

Fig. 1. Particle size distribution of PPT-SS and SS batches obtained by sonocrystallization at constant temperature, concentration and varied amplitude. Samples were taken at 3 min.

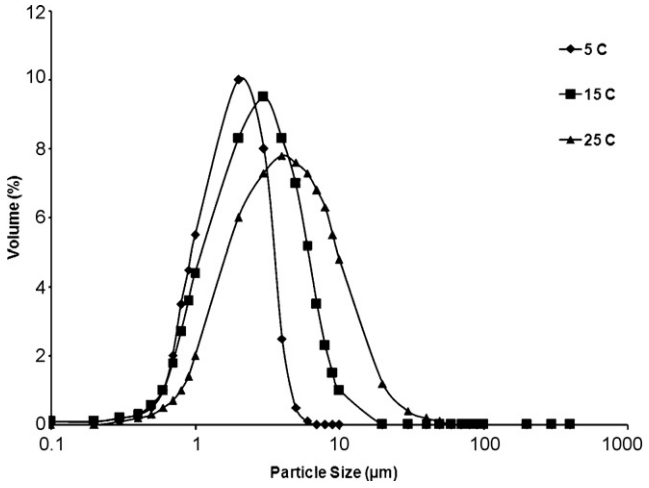

Fig. 2. Particle size distribution of SS obtained by sonocrystallization at constant amplitude, concentration and varied temperature. Samples were taken at 3 min.

A range of temperatures was also tested in Batches 2, 4 and 5, sonicated for 3 min after addition of 250 mg/ml SS solution. The effect of temperature on size distribution is shown in Fig. 2. It was observed that at lower temperatures the distribution shifts towards lower size with smaller span values indicting narrow size distributions. Both span and particle size were lowest at temperature of 5 °C. Decrease in the solubility of SS in aqueous-ethanol solution at lower temperature might have resulted in early supersaturation and nucleation which might have favored the formation of fine particles. All further experiments were carried out at 5 °C and 50% amplitude.

Effect of sonication time in the range of 1–5 min (Batches 2, 6 and 7) on the PSD is shown in Fig. 3. Batch 6, with 1 min sonication time showed wider size distribution. When the time of sonication was increased to 3 min, VMD and span were found to decrease. No difference was observed in particle size and span values after increasing the sonication time from 3 min (Batch 2) to 5 min (Batch 7). At shorter period of exposure (1 min), rapid nucleation occurred, followed by crystal growth and agglomeration. However, sonication time of 3 min was enough to reduce growth and agglomeration of crystals. The complete liberation of supersaturation has occurred

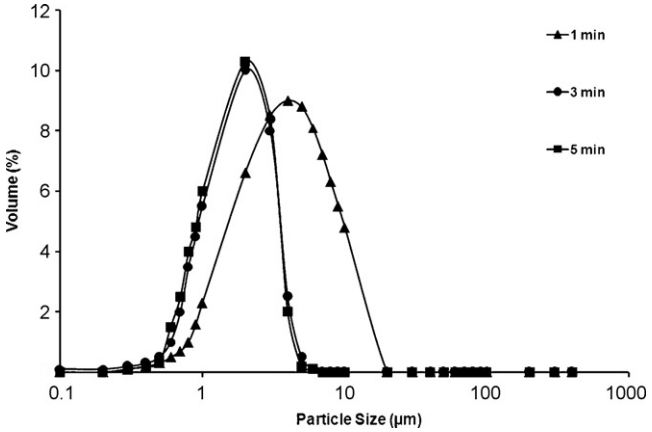

Fig. 3. Particle size distribution of SS obtained by sonocrystallization at constant temperature, amplitude, concentration and varied time.

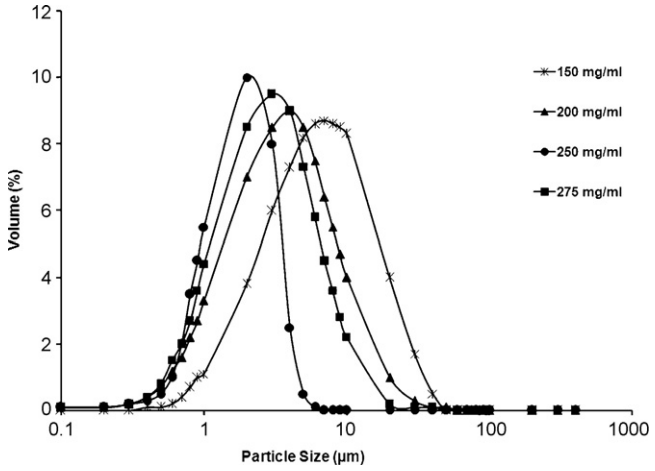

Fig. 4. Particle size distribution of SS obtained by sonocrystallization at optimum amplitude, temperature and varied concentration. Samples were taken at 3 min.

in 3 min and hence, increase in the sonication time to 5 min did not show any further alteration in VMD and span. Therefore, sonication time of 3 min was considered to be optimum.

Effect of the concentration of SS solution was evaluated between 150 and 275 mg/ml. As shown in Fig. 4, the crystal size and span values were found to reduce with increase in the SS concentration up to 250 mg/ml. This is because higher the concentration of SS, closer is the concentration to the supersaturation point and higher the driving force for nucleation. However, we observed a reverse in the trends when concentration was increased from 250 to 275 mg/ml in water. At this higher concentration, the higher span was observed with large size range compared to 250 mg/ml. When highly supersaturated conditions are achieved rapidly by mixing solution with anti-solvent, few local zones of excessive supersaturations may be generated leading to agglomeration of nuclei before ultrasound provides uniform microscopic mixing by vibration and cavitation throughout the vessel. Though further nucleation and crystal growth takes place homogeneously under the influence of ultrasound, the crystals grown on the already agglomerated nuclei contribute for higher values of span. It can therefore be inferred that 250 mg/ml concentration of SS solution was found to be optimum.

Batch 2 showed smallest particle size (VMD, 1.8 μm) and span indicating optimum operating conditions. Since crystallization in highly supersaturated solutions is uncontrollable by conventional methods as observed in PPT-SS, insonation plays a vital role for generating crystals with desired particle size. SCSS dispersion of optimum batch (Batch 2) was spray dried to separate the SS crystals in dry and free flowing form. The effect of spray drying on the PSD of crystals was studied by laser diffraction. Spray drying resulted in slight reduction of VMD (1.6 μm). This might be due to high shear at the nozzle during spray drying. SDSS obtained by spray drying aqueous solution of SS showed VMD of 3.1 μm with narrow PSD as studied by laser diffraction and is in accordance with that reported by Chawla et al. (1994). Infra red spectra of unprocessed SS, PPT-SS, SDSS and SD-SCSS were similar suggesting no change in the chemical structure of SS on either anti-solvent crystallization, sonocrystallization or spray drying.

3.1.2. Particle morphology

The SEM images of unprocessed SS, micronized SS, PPT-SS, SDSS, SCSS, and SD-SCSS are shown in Fig. 5. The SEM image of unprocessed SS showed large crystalline particles with few microparticles in the size range of 2–50 μm. Micronized SS showed the agglomerated particles in the size range below 5 μm. While, SDSS showed uniform, spherical particles in the size range below 5 μm. Some pitting and shrunken areas were observed on the surface of SDSSS particles. The SEM image of PPT-SS showed the agglomerates of large and small crystals of irregular shape. SEM images of SCSS before spray drying exhibited elongated, needle shaped crystals having approximately 0.1–0.3 μm width and 0.5–2.5 μm length. In the present study, uniform superstaurated conditions were achieved rapidly throughout the crystallization vessel with ultrasonic insonation resulting in rapid crystallization. Ultrasound is known to increase or decrease the growth rate of certain crystal faces (Guo et al., 2005). When lactose is crystallized rapidly it appears to accelerate the growth of longest axis of the crystals at the expense of an increase in width and thickness resulting in needle-shaped, elongated crystals (Larhrib et al., 2003a; Dhumal et al., 2008a). Moreover, if the growth takes place preferentially in the longitudinal direction, drug particles can have similar thickness. Therefore, a powder with a narrower distribution can be obtained. SD-SCSS showed needle shaped micro-crystals of SCSS forming loose oval aggregates measuring around 3–7 μm in size due to instantaneous drying of spherical droplets containing micro-crystals.

3.1.3. Powder flow

Spray drying the SCSS dispersion resulted in loose oval aggregates with much lower tapped density (0.2 g/cm^3) compared to micronized SS (0.5 g/cm^3) and unprocessed SS (0.8 g/cm^3). This indicates the non-isometric shape of SD-SCSS crystals, which were unable to pack effectively. This finding is in agreement with SEM images showing elongated shape of crystals forming loose aggregates of oval shape (Fig. 5). Moreover, owing to oval shape, the loose aggregates were able to flow effectively as indicated by the lower values of Carr's index for SD-SCSS (CI, 16 ± 1) than SDSS (CI, 19 ± 1) and micronized SS (CI, 23 ± 1).

3.2. Characterization of polymorphic form

The polymorphic form of the drug before and after processing was characterized by DSC and XRPD. The DSC thermogram of unprocessed SS showed sharp endothermic peak at 200 °C, which was related to the melting of SS (Fig. 6). This peak is recently ascribed to melting with decomposition of SS (Larhrib et al., 2003b). Crystalline nature of unprocessed SS was confirmed by sharp diffraction peaks in XRPD patterns (Fig. 7). The XRPD spectra of SD-SCSS was similar to unprocessed SS showing presence of sharp diffraction peaks demonstrating crystalline nature of drug particles. This finding was supported by the endothermic peak corresponding to melting of SS at 200 °C in the thermogram of SD-SCSS, confirming the crystalline nature of SS obtained by sonocrystallization followed by spray drying. However, thermogram of SDSS obtained by spray drying aqueous solution of SS did not show the melting transition; instead a T_g appeared at ~64 °C. This clearly indicated the existence of amorphous state of the drug, which was also confirmed by XRPD showing a halo, characteristic to amorphous form. These results were similar to Chawla et al. (1994). In SD-SCSS, spray-drying was not used to form particles as if solutions were to be dried, but to dry the dispersion of pre-formed crystals. Therefore, in this study, spray drying had resulted in crystalline SS.

3.3. Stability studies

The polymorphic form of SDSS and SD-SCSS on storage at 40 °C/75% RH was monitored by DSC and XRPD after regular interval. Stability samples of SD-SCSS after storage for 1, 2 and 3 months

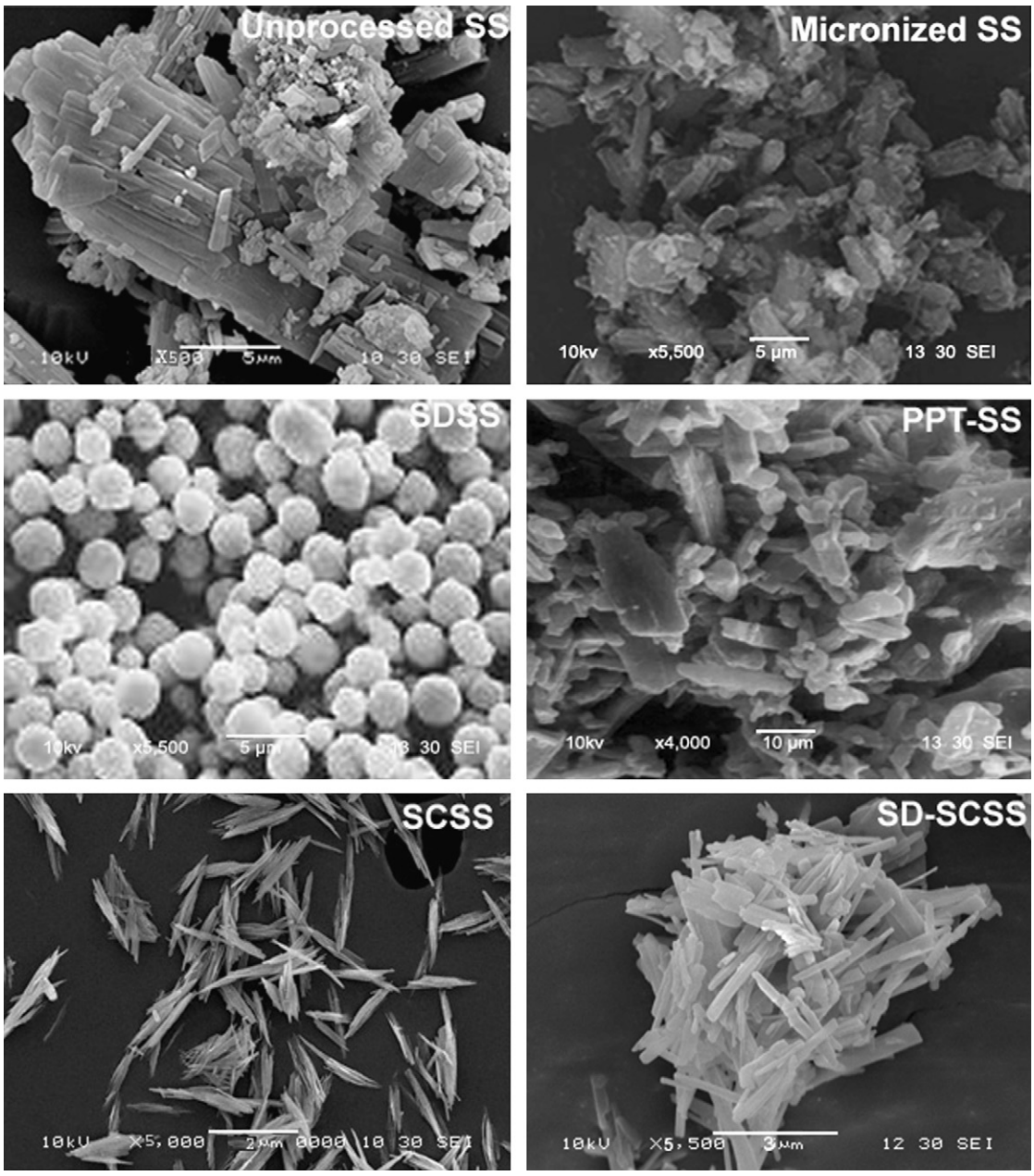

Fig. 5. SEM photomicrographs of unprocessed SS, micronized SS, SDSS, SCSS dispersion of Batch 2 evaporated on glass slide, PPT-SS and SD-SCSS.

do not show any difference in the DSC and XRPD pattern with respect to initial sample indicating no change in crystallinity. Since there was no difference in stability samples, results of only 3-month stability sample are shown in Figs. 6 and 7. However, SDSS showed gradual gain in crystallinity on storage at 40 °C/75% RH as observed in DSC thermograms and XRPD patterns with 3-month stability sample showing crystallinity nearly identical with the unprocessed crystalline sample (Figs. 6 and 7). Amorphous drugs are thermodynamically unstable and tendency of amorphous SS to absorb moisture, agglomerate and recrystallize on storage is already reported (Buckton et al., 1995). As expected, SD-SCSS was less hygroscopic as indicated by no significant change in moisture content on storage for 3 months (initial, 0.36 ± 0.01%, w/w and 3 months, 0.39 ± 0.02%, w/w), but SDSS showed increase in moisture content from 0.61 ± 0.02% (w/w) to 2.38 ± 0.04% (w/w) after 3 months.

3.4. Aerosol performance

Micronized SS, SDSS and SD-SCSS samples were blended with CL in a ratio of 1:67.5 and filled in hard gelatin capsule. The content uniformity ranged from 96.13 ± 0.67 to 99.34 ± 0.83% for all samples. The *in vitro* aerosol deposition studies were carried out in cascade impactor using Rotahaler® at 28.3 l/min and the data is recorded in Table 2. The drug recovery for formulations ranged from 95 ± 1.1 to 97 ± 1.3%, which was within the acceptable range (75–125%) for mass balance (Bryon et al., 1994) and also suggested that the method of washing and analyzing was accurate and reproducible. The percent mass deposited on different stages of cascade impactor from micronized SS, SDSS and SD-SCSSS are shown in Fig. 8. Micronized SS showed lower FPF (16.66 ± 1.9%) which is in accordance with earlier studies. The marketed products based on micronized SS have also shown lower FPF's due to cohesive

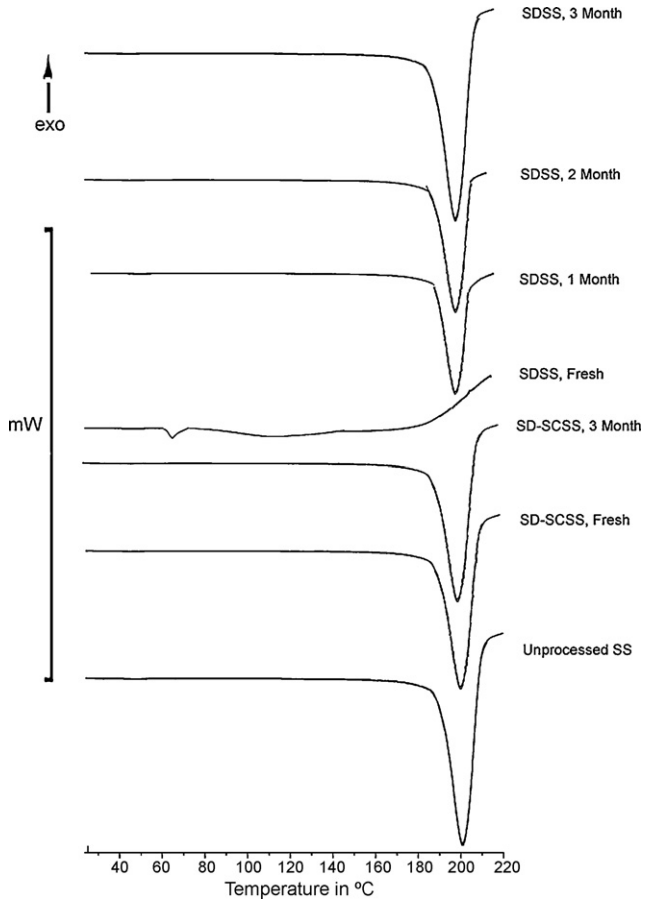

Fig. 6. DSC thermograms of unprocessed SS, fresh and stability samples of SDSS and SD-SCSS.

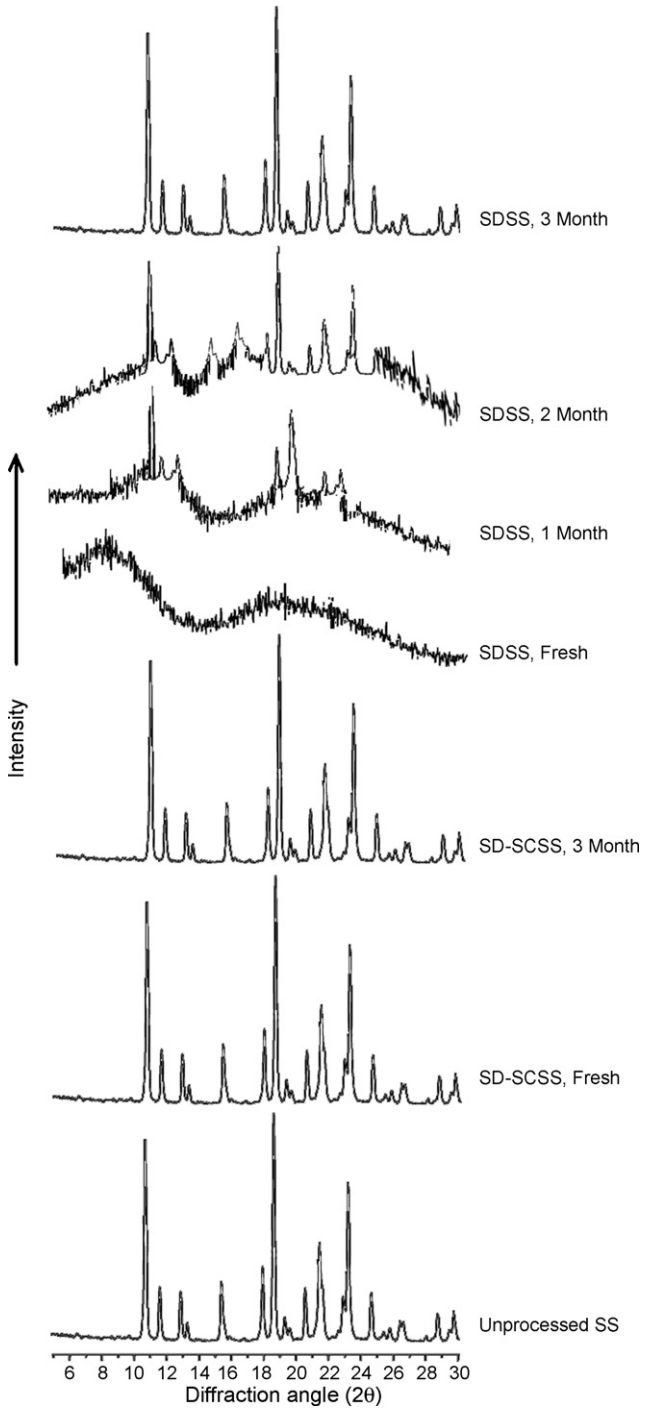

Fig. 7. XRPD patterns of unprocessed SS, fresh and stability samples of SDSS and SD-SCSS.

nature of micronized SS (Newman et al., 1981). While SDSS showed improved FPF ($31.12 \pm 1.6\%$) compared to micronized SS. This can be also noted from Fig. 8 which indicates higher impaction loss of micronized SS in induction port and preseparator, along with a subsequent decrease in deposition on stages 2–7 in the cascade impactor compared to SDSS. This improvement in deposition profile of SDSS may be due to spherical nature of particles with uniform size distribution and pitted surface with fewer points of contact exhibiting better de-agglomeration from carrier.

The aerosol performance of SD-SCSS formulation indicates lowest impaction loss and highest FPF ($44 \pm 1.5\%$) with decreased drug loss in induction port and preseparator, along with a subsequent increase in deposition on stages 2 and below of cascade impactor (Fig. 8). The reason for improved performance of SD-SCSS may be, the reduced cohesive and adhesive forces in interactive mixture resulting in better flow and de-agglomeration from the surface of carrier. The elongated, needle shape of individual crystals prevents close packing between the crystals, which effectively increases the inter-particulate distance and lowers the van der Waals attractive forces giving loose aggregates as confirmed from SEM images and

Table 2
Deposition of SS from SDSS and SD-SCSS formulations with CL in cascade impactor at 28.3 l/min via Rotahaler® (mean (S.D.), $n = 3$).

Batch code	RD (μg)	ED (μg)	FPD (μg)	FPF (%)	Recovery (%)	Emission (%)	MMAD (μm)	GSD
Micronized SS	429 (17)	284 (15)	71.5 (11)	16.66 (1.9)	89.18 (1.6)	59.04 (1.9)	7.16 (0.21)	1.91 (0.08)
SDSS, fresh	458 (16)	328 (14)	142 (11)	31.12 (1.6)	95.21 (1.8)	68.19 (2.1)	6.46 (0.11)	1.89 (0.08)
SDSS, 3 months	429 (21)	289 (19)	81.5 (13)	18.99 (1.9)	90.00 (1.9)	60.08 (1.9)	6.56 (0.21)	1.91 (0.09)
SD-SCSS, fresh	473 (11)	359 (10)	209 (7)	44.21 (1.3)	98.33 (1.3)	74.63 (1.4)	3.82 (0.12)	1.77 (0.09)
SD-SCSS, 3 months	465 (13)	355 (12)	207 (8)	44.08 (1.5)	96.67 (1.4)	73.38 (1.6)	3.71 (0.11)	1.82 (0.10)

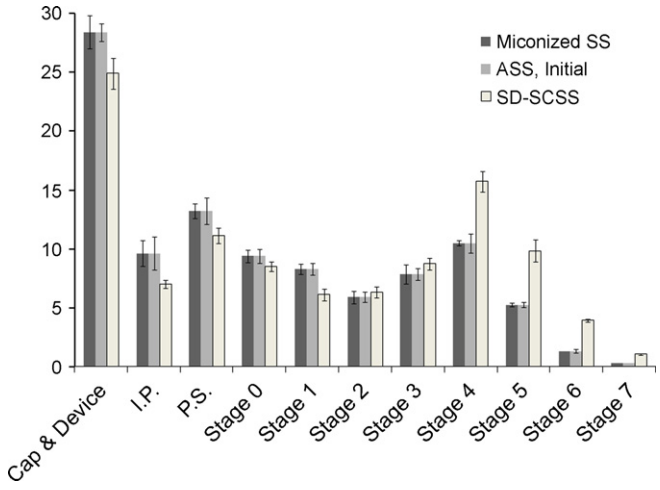

Fig. 8. Drug deposition profiles of micronized SS, SDSS and SD-SCSS formulations with CL in Andersen cascade impactor at 28.3 l/min via Rotahaler®. $n = 3$.

density values. During mixing of SD-SCSS with CL the loose aggregates break down into individual crystals by the shear forces from the collisions between the agglomerates and the carrier. Thus, individual crystals and not the aggregates adhere to the carrier surface as seen from SEM image of the SD-SCSS formulation with CL in Fig. 9. In contrast, micronized drugs are reported to adhere to the carrier surface as aggregates owing to its activated surface and cohesive nature. The elongated shape of SD-SCSS crystals are known to reduces the effective areas of contact between the crystals and the carrier surface reducing the adhesive forces (Ikegami et al., 2002; Larhrib et al., 2003a). Traditionally, non-spherical particles have been avoided for potential problems of powder flow. However, the respirable fraction of drugs is shown to improve with the elongation ratio of drug (Ikegami et al., 2002) and carrier (Dhumal et al., 2008a; Larhrib et al., 2003a). SD-SCSS produced MMAD of 3.82 μm with 1.77 ± 0.09% GSD, because for elongated particles, aerodynamic diameter shows a relatively small dependence on the length but is strongly correlated to the short dimension of the particles. The rod thickness is taken into account to calculate the aerodynamic diameter of the powder.

The samples of SDSS and SD-SCSS after subjecting to 3 months stability conditions were blended with CL and studied for *in vitro* deposition studies. The stability sample of SDSS showed poor

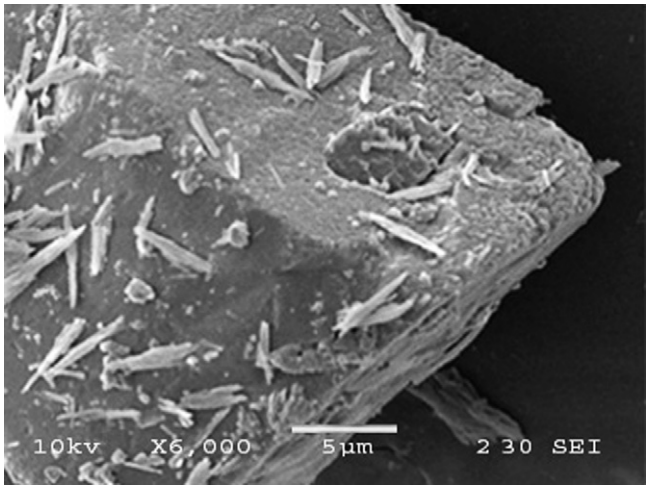

Fig. 9. SEM photomicrogrph of the surface of SD-SCSS formulation with CL.

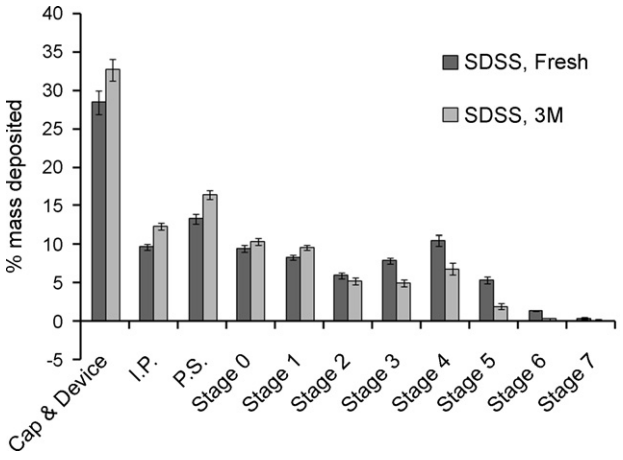

Fig. 10. Drug deposition profiles of fresh and stability samples of SDSS formulation with CL in Andersen cascade impactor at 28.3 l/min via Rotahaler®. $n = 3$.

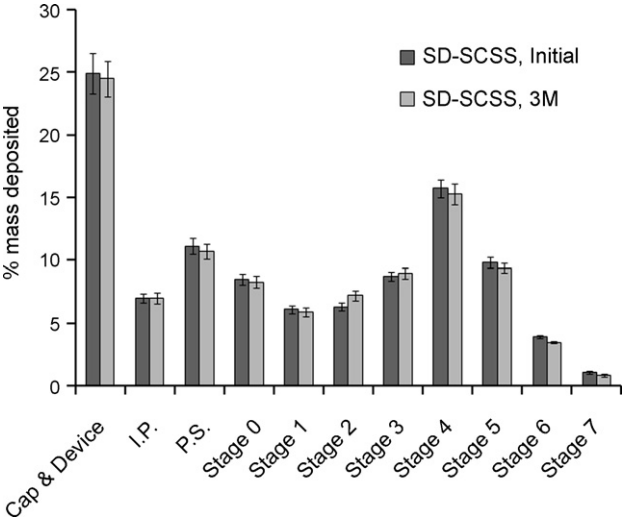

Fig. 11. Drug deposition profiles of fresh and stability samples of SD-SCSS formulation with CL in Andersen cascade impactor at 28.3 l/min via Rotahaler®. $n = 3$.

deposition profiles (Fig. 10 and Table 2). This was due to the recrystallization of amorphous SS on storage at high temperature and humidity with further increase in moisture content and agglomeration indicating unstability and non-suitability of amorphous systems for pulmonary delivery in the form of DPI. However, no significant difference was observed in the deposition profiles of SD-SCSS with respect to fresh sample (Fig. 11 and Table 2). This was due to the physical stability of the microcrystals obtained in respirable size by sonocrystallization as confirmed by results of DSC and XRPD studies.

4. Conclusion

Sonocrystallization; a rapid crystallization technique was developed for engineering elongated needle shape crystals of SS in respirable size with narrow size distribution. With cavitation and acoustic streaming, ultrasound shows a great ability in blending of the anti-solvent with the SS solution resulting in uniform and rapid nucleation followed by more rapid crystallization forming elongated fine crystals with uniform size compared to anti-solvent crystallization without sonication, which resulted in agglomerates of large crystals with irregular shape. Higher sonication amplitude and concentration with lower temperatures favored formation of

smaller crystals with narrow size distribution. Spray drying was used for obtaining dry crystalline powder with improved FPF and stability compared to micronized SS and amorphous SS. Moreover, amorphous SS destabilized on storage and showed poor deposition profile. The elongated nature of crystals reduces the effective areas of contact between the crystals and the carrier surface reducing the adhesive forces to produce smaller aerodynamic size and better FPF. Hence, this study has demonstrated sonocrystallization as potential particle engineering technique for preparing stable micro-crystals with size and shape suitable for pulmonary delivery.

Acknowledgements

Anant R. Paradkar is thankful to British Council for UK-India Education and Research Initiative (UKERI) Fellowship, Bharati Vidyapeeth University, Pune for the sabbatical leave and AICTE (New Delhi, India) for grant in the form of Research Promotion Scheme. Ravindra S. Dhumal and Shailesh V. Biradar are thankful to CSIR (New Delhi, India) for providing financial support in the form of senior research fellowship (SRF). The authors are thankful to Prof. A. N. Misra, Pharmacy Department, Faculty of Technology and Engineering, The Maharaja Sayajirao University of Baroda, Vadodara, India for providing the facilities of Andersen cascade impactor. Authors acknowledge the support of Cipla Ltd. (Mumbai, India), DMV International (The Netherlands) and Universal Capsules (Mumbai, India) for providing gift samples of salbutamol sulphate, lactose monohydrate and hard gelatin capsules, respectively.

References

Ambike, A.A., Mahadik, K.R., Paradkar, A., 2004. Stability study of amorphous valdecoxib. Int. J. Pharm. 282, 151–162.

Blagden, N., de Matas, M., Gavan, P.T., York, P., 2007. Crystal engineering of active pharmaceutical ingredients to improve solubility and dissolution rates. Adv. Drug Deliv. Rev. 59, 617–630.

Briggner, L.E., Buckton, G., Bystrom, K., Darcy, P., 1994. The use of isothermal microcalorimetry in the study of changes in crystallinity induced during the processing of powders. Int. J. Pharm. 105, 125–135.

Bryon, P.R., Kelly, E.L., Kontny, M.J., 1994. Recommendations of the USP Advisory Panel on aerosols on the USP general chapters on aerosols ⟨6 0 1⟩ and uniformity of dosage units ⟨9 0 5⟩. Pharm. Forum 20, 7477–7505.

Buckton, G., Darcy, P., Greenleaf, D., Holbrook, P., 1995. The use of isothermal microcalorimetry in the study of changes in crystallinity of spray-dried salbutamol sulphate. Int. J. Pharm. 116, 113–118.

Chawla, A., Taylor, K.M.G., Newton, J.M., Johnson, M.C.R., 1994. Production of spray-dried salbutamol sulfate for use in dry powder aerosol formulation. Int. J. Pharm. 108, 233–240.

Dhumal, R.S., Biradar, S.V., Paradkar, A.R., York, P., 2008a. Ultrasound assisted crystallization of lactose crystals. Pharm. Res. 25, 2835–2844.

Dhumal, R.S., Biradar, S.V., Yamamura, S., Paradkar, A.R., York, P., 2008b. Preparation of amorphous cefuroxime exetil nanoparticles by sonoprecipitation for enhancement of bioavailability. Eur. J. Pharm. Biopharm. 70, 109–115.

Guo, Z., Zhang, M., Li, H., Wang, J., Kougoulos, E., 2005. Effect of ultrasound on anti-solvent crystallization process. J. Crystal Growth 273, 555–563.

Hu, J., Rogers, T.L., Brown, J., Young, T., Johnson, K.P., Wolliams, R.O., 2002. Improvement of dissolution rates of poorly water soluble APIs using novel spray freezing into liquid technology. Pharm. Res. 19, 1278–1284.

Ikegami, K., Kawashima, Y., Takeuchi, H., Yamamoto, H., Isshiki, N., Momose, D., Ouchi, K., 2002. Improved inhalation behavior of steroid KSR-592 *in vitro* with Jethaler® by polymorphic transformation to needle-like crystals (β-form). Pharm. Res. 19, 1439–1445.

Kaerger, J.S., Price, R., 2004. Processing of spherical crystalline particles via a novel solution atomization and crystallization by sonication (SAXS) technique. Pharm. Res. 21, 372–381.

Larhrib, H., Martin, G.P., Prime, D., Marriot, C., 2003a. Characterization and deposition studies of engineered lactose crystals with potential for use as a carrier for aerosolized salbutamol sulphate from dry powder inhalers. Eur. J. Pharm. Sci. 19, 211–221.

Larhrib, H., Martin, G.P., Marriot, C., Prime, D., 2003b. The influence of carrier and drug morphology on the drug delivery from dry powder formulations. Int. J. Pharm. 257, 283–296.

Louhi-Kultanen, M., Karjalainen, M., Rantanen, J., Huhtanen, M., Kallas, J., 2006. Crystallization of glycine with ultrasound. Int. J. Pharm. 320, 23–29.

Luque de Castro, M.D., Priego-Capote, F., 2007. Ultrasound-assisted crystallization (sonocrystallization). Ultrason. Sonochem. 14, 717–724.

Maheshwari, M., Jahagidar, H., Paradkar, A.R., 2005. Melt sonocrystallization of ibuprofen: effect on crystal properties. Eur. J. Pharm. Sci. 25, 41–48.

Newman, S.P., Pavia, D., Moren, F., Sheahan, N.F., Clarke, S.W., 1981. Deposition of pressurized aerosols in the human respiratory track. Thorax 36, 52–55.

Nocent, M., Bertocchi, L., Espitalier, F., Baron, M., Courraze, G., 2001. Definition of a solvent system for spherical crystallization of salbutamol sulfate by quasi-emulsion solvent diffusion (QESD) method. J. Pharm. Sci. 90, 1620–1627.

Paradkar, A., Maheshwari, M., Kamble, R., Grimsey, I., York, P., 2006. Design and evaluation of celecoxib porous particles using melt sonocrystallization. Pharm. Res. 23, 1395–1400.

Schiavone, H., Palakodaty, S., Clark, A., York, P., Tzannis, S.T., 2004. Evaluation of SCF-engineered particle-based lactose blends in passive dry powder inhalers. Int. J. Pharm. 281, 55–66.

Ticehurst, M.D., Basford, P.A., Dallman, C.I., Lukas, T.M., Marshall, P.V., Nichols, G., Smith, D., 2000. Characterisation of the influence of micronisation on the crystallinity and physical stability of revatropate hydrobromide. Int. J. Pharm. 193, 247–259.

Waltersson, J.O., Lundgren, P., 1985. The effect of mechanical comminution on drug stability. Acta Pharm. Suec. 22, 291–300.

York, P., 1999. Strategies for particle design using supercritical fluid technologies. Pharm. Sci. Technol. Today 2, 430–440.

Zeng, X.M., Martin, G.P., Marriott, C., Pritchard, J., 2001. The use of lactose recrystallised from carbopol gels as a carrier for aerosolised salbutamol sulphate. Eur. J. Pharm. Biopharm. 51, 55–62.